Title:

A comparison of the relative effect of the Earth's Quasi-D.C. and A.C. electric field on Gradient Drift Waves in large-scale plasma structures in the polar regions.

Authors:

Robert Burston, Department of Electronic and Electrical Engineering, The University of Bath, Claverton Down, Bath, UK.

Cathryn Mitchell, Department of Electronic and Electrical Engineering, The University of Bath, Claverton Down, Bath, UK.

Ivan Astin, Department of Electronic and Electrical Engineering, The University of Bath, Claverton Down, Bath, UK.

Corresponding author: I. Astin, Department of Electronic and Electrical Engineering, The University of Bath, Claverton Down, Bath, BA27AY, UK. (eesia@bath.ac.uk)

Key Points.

Using DE2 data, the relative strengths of A.C. and D.C. electric field components in large-scale plasma structures in polar regions are compared

In such data, the order of magnitude of A.C. component is found to be greater than the D.C. component in 60% of cases

This implies that gradient drift waves are not confined to the trailing edge such structures

This article has been accepted for publication and undergone full peer review but has not been through the copyediting, typesetting, pagination and proofreading process which may lead to differences between this version and the Version of Record. Please cite this article as doi: 10.1002/2016JA022676

Abstract

Radio signals traversing polar-cap plasma patches and other large-scale plasma structures in polar regions are prone to scintillation. This implies that irregularities in electron concentration often form within such structures. The current standard theory of the formation of such irregularities is that the primary Gradient Drift Instability drives a cascade from larger to smaller wavelengths that manifest as variations in electron concentration. The electric field can be described as the sum of a quasi-D.C. and an A.C. component. Whilst the effect of the quasi-D.C. component has been extensively investigated in theory and by modelling, the contribution of the A.C. component has been largely neglected. This paper investigates the relative contributions of both components, using data from the Dynamics Explorer 2 satellite. It concludes that the contribution of the A.C. electric field to irregularity growth cannot be neglected. This has consequences for our understanding of large-scale plasma structures in polar regions (and any associated radio scintillation) as the A.C. electric field component varies in all directions. Hence, it effect is not limited to the trailing edge of such structures, as it is for the quasi-D.C. component. This raises the need for new experimental and modelling investigations of these phenomena.

Introduction

[*Hill* (1963)] theorized that high latitude sporadic-F events, as recorded with analogue ionosondes, were caused by plasma enhancements in the polar-cap ionosphere convecting according to an $\mathbf{E} \times \mathbf{B}$ drift, caused by the combination of the Earth's magnetic field **B** and an electric field **E** mapped from the magnetosphere. Direct confirmation of this theory came with all sky images reported in [*Buchau et al.* (1983)], that showed just such enhancements, now generally known as polar-cap plasma patches. A correlation between radio signal ray-paths transecting polar-cap plasma patches and UHF scintillation of the signal received at the ground was demonstrated soon after [*Weber et al.*, 1984]. Scintillation associated with

plasma patches has been found to occur across a wide range of radio frequencies including GNSS [e.g. *Jin et al.*, 2014].

Ionospheric scintillation is the phenomenon of rapid phase or amplitude fluctuations of a received signal, induced during passage of the signal through the ionosphere [*Kintner et al.*, 2007]. For scintillation, the mechanism is propagation of the signal through "irregularities" in the ionospheric electron density. Such irregularities give rise to variations in the refractive index of the ionosphere that causes the scintillation [e.g. *Hargreaves*, 1992; *Hunsucker and Hargreaves*, 2002].

A number of explanations for the mechanism of irregularity formation within polar-cap plasma patches and large-scale plasma structures in the polar regions have been proposed, including the Current Convective Instability (CCI), first suggested in relation to auroral structures [*Ossakow and Chaturvedi*, 1979] and in plasma patches by *Kelley* (2009), the primary Kelvin-Helmholtz Instability (KHI) (possibly in conjunction with other processes) [e.g. *Carlson et al.*, 2007; *Gondarenko and Guzdar*, 2006; *Oksavik et al.*, 2012] , the Gradient Drift Instability (GDI) [e.g. *Basu et al.*, 1990; *Burston et al.*, 2009; *Chaturvedi et al.*, 1994; *Gondarenko, and Guzdar*, 2006; *Kivanc and Heelis*, 1997; *Weber et al.*, 1984] and a related 'Turbulent" process [*Kelley and Kintner*, 1978], which we term Kelley-Kintner-Turbulence (KKT). The term 'turbulence' comes from magnetospheric electric fields that are "turbulent" in that they show continual variation at short time scales, and these fluctuations are also mapped to the ionosphere, exposing plasma to rapidly varying $\mathbf{E} \times \mathbf{B}$ drifts that can cause gradient drift instabilities, generating turbulent mixing of the plasma, if there is an electron concentration gradient present [*Burston et al.*, 2010, *Kelley*, 1989].

Using Dynamics Explorer 2 satellite observations [*Burston el al.*, 2016] investigated the range of possible values for the linear growth-rates for each of these processes. In that study, we found that the inertial KKT instability gave rise to the largest growth rates followed by those for inertial Gradient Drift, collisional Turbulence and collisional shortwave Current Convective instabilities. Growth rates for the primary KHI (in agreement with [*Oksavik et al.*, 2012]) were found to be far too small to be significant, as were the growth rates for the long wavelength CCI. These results, and similarities between the GDI and KKT, have inspired this follow-up study. In particular, the GDI requires an electric field perpendicular to a gradient in plasma concentration and a magnetic field perpendicular to both in order to occur. A pre-existing perturbation in the plasma concentration gradient is also required. All these conditions can be met in the case of large-scale plasma structures in the polar regions since the geo-magnetic field is approximately vertical and there must be an appreciable electric field mapped from the magnetosphere to the ionosphere or the patch could not be convecting via an $\mathbf{E} \times \mathbf{B}$ drift force and hence would not exist. The growth rate for the GDI [*Linson and Workman*, 1970] are as follows:

$$\gamma_{cGDI} = \frac{\mathbf{E} \times \mathbf{B}}{B^2}\left(\frac{\nabla n}{n}\right) \quad [1]$$

(collisional regime) and

$$\gamma_{iGDI} = \left[\nu_{in}\frac{\mathbf{E} \times \mathbf{B}}{B^2}\left(\frac{\nabla n}{n}\right)\right]^{1/2} \quad [2]$$

(inertial regime), where $\mathbf{E}$ is the electric field strength, $\mathbf{B}$ is the magnetic field strength, n is the free electron concentration and ν_{in} is the ion-neutral collision frequency [e.g. *Sojka et al.*, 1998]. The subscripts *c* and *i* denote the collisional and inertial regimes, respectively. The cut-off between the two regimes is where the collisional rate and collisional regime growth rate become equal in value. In these equations $\mathbf{E}$ is usually considered to be the quasi-D.C. component of the magnetosphere-to-ionosphere mapped electric field. In other words, short time-scale fluctuations in the direction and magnitude of the field are ignored. It is possible to

derive equations that take account of the A.C. component of the field, separately, by replacing **E** with

$$\left[\int_{k_L}^{\infty} E(k)^2\, dk\right]^{1/2} \quad [3]$$

which represents the root-mean-squared electric field strength due to the A.C. variations in the field with wavenumbers from k_L to infinity, where k_L is the smallest relevant wavenumber, in this case $k_L = 2\pi(\nabla n/n)$ where $(n/\nabla n)$ is the scale of the structure.

Substituting Eq.[3] into Eqs.[1] and [2] yields,

$$\gamma_{cT} = \left[\int_{k_L}^{\infty} E(k)^2\, dk\right]^{1/2} \left(\frac{|\nabla n|}{nB}\right) \quad [4]$$

and

$$\gamma_{iT} = \left\{\nu_{in}\left[\int_{k_L}^{\infty} E(k)^2\, dk\right]^{1/2} \left(\frac{|\nabla n|}{nB}\right)\right\}^{1/2} \quad [5]$$

respectively. These ideas and Eqs.[3-5] were presented in [*Kelley and Kintner* (1978)]. The subscript *T* is used for these growth-rates, as these refer to Kelley-Kintner 'Turbulence'.

The GDI and Kelley-Kintner Turbulence (KKT) give rise to growth rate equations that are similar in form. However, the differences between the electric fields driving them lead to the possibility of different effects. In Eqs.[1] and [2] the fields are vector quantities and consequently the instability can only initiate on the trailing edge. Eqs.[4] and [5] are *not* vector relations, as the A.C. component of the electric field has no directional bias and fluctuates in all directions. Since there is also a gradient in electron concentration in all directions, this process is always viable in some direction and is not confined to the trailing edge. As the only difference between the GDI and KKT equations is the electric field term, it is possible to assess which process likely dominates simply by dividing one by the other. In particular, both Eq.[1] ÷ Eq.[4] and Eq.[2]÷ Eq.[5] yield

$$\mathbf{E}/\left[\int_{k_L}^{\infty} E(k)^2\, dk\right]^{1/2} \quad [6]$$

which we re-define as E_{DC}/E_{AC} for simplicity, since henceforth only the relative magnitudes are important. It should be noted that two or three dimensional growth-rate equations and non-linear damping terms are unimportant here, since they will be identical for both the GDI and KKT cases except for the electric field values. Hence E_{DC}/E_{AC} can be used as a theoretically measure of which process dominates at any given time. If $E_{DC}/E_{AC} > 1$, the GDI likely dominates, if $E_{DC}/E_{AC} < 1$, then KKT likely dominates and if $E_{DC}/E_{AC} \approx 1$ neither dominates.

For example, this has implications with regard to observations about the spatial structuring of patches. In particular, [*Kivanc and Heelis* (1997)] used Dynamics Explorer satellite data to classify patches into four types according to their internal irregularity structure distributions. These classes were: 1) no structuring, 2) structuring only on the trailing edge, 3) structuring through-out the patch and 4) structuring on the trailing and leading edges. Class one can be explained as having no instability operating or the instability operating for too short a time when the observations were made. Classes two and three can be explained by the GDI at earlier and later stages of growth respectively. Class four can only be explained by the GDI if the direction of motion of the patch has altered radically, so that what was the trailing edge is now effectively the leading edge and vice versa. This was demonstrated by modelling [*Gondarenko et al.,2003*]. A simpler explanation would be that the KKT process is operating on all gradients at an appreciable rate. This could also explain the creation of fully structured patches (class three) at a rate faster than the GDI alone could produce as irregularities would only have to grow to the patch radius rather than the patch diameter for the case of the GDI alone.

A sufficient number of observations of E_{DC}/E_{AC} would therefore indicate statistically whether KKT is likely to be a significant irregularity generating process. This experiment was performed using data from the Dynamics Explorer 2 (DE2) satellite's Vector Electric Field Instrument (VEFI). Results show that E_{AC} is of the same order of magnitude or greater than E_{DC} in 94% of the large-scale plasma structures cases identified in the polar regions. It is therefore concluded that KKT is likely a significant process in plasma patches and that the contributions of the A.C. fluctuations of the mapped electric field must be taken into account to fully understand plasma structuring, particularly with regard to plasma patches showing structure on both trailing and leading edges and fully structured patches.

Method

The Dynamics Explorer 2 satellite [http://nssdc.gsfc.nasa.gov/nmc/experimentDisplay.do?id=1981-070B-09], launched in August 1981 and re-entering in February 1983, flew in an elliptical, polar orbit, allowing it to make observations of the ionosphere above both polar caps. On board was the Vector Electric Field Instrument (VEFI) which consisted of three mutually perpendicular instruments capable of measuring electric field strength and allowing for recovery of the full vector electric field strength, **E**. This included separate measurements of both the quasi-D.C. and the A.C. components of the field up to 1024 Hz [*Heppner et al.*, 1978a; *Heppner et al.*, 1978b]. In particular, the quasi-D.C is the short duration component of the Earths electric field < 4 Hz and the AC is the rest (4 Hz - 1024 Hz). This quasi-D.C. component is stationary in time (over short-time scales < 1 min), but is not stationary in space.

Since the interest here is the electric field within large-scale plasma structures in the polar regions all measurements below 65° magnetic latitude (for each hemisphere) were excluded. Secondly, data above 400 km were excluded to eliminate data from far above the F-peak. The retained data are all in the range 300-400 km, as DE2 never descended below 300 km during routine operation. Thirdly, a method of identifying gradients in electron concentration was adopted as follows. Orbit segments with an electron concentration gradient of 40% or greater across the whole of a 140 km± 5% orbit segment were retained. Figure 1 shows the electron concentration, the quasi-D.C. (x and y) components and the power spectra of the individual A.C. (x and y) components for an example orbit segment (meeting the above three criteria).

Because of the retention of only high-latitude data, the probable sources of gradients in electron concentration are only auroral structures and plasma patches. Since the steep gradients retained are calculated across 140 km orbit segments as a whole, not within them, it is unlikely that they are auroral in origin. This method was first used by [Coley and Heelis, 1995] and recently used by [*Burston et al.*, 2016] across a wider magnetic latitude. It should be noted that some retained orbit segments may overlap others. The data used to calculate the electron concentration gradients were taken from the DE2 Langmuir probe experiment. Strictly, as the gradient should be determined along its steepest direction rather than the satellite track this would tend to lead to an underestimate of the actual gradient.

The mean values of E_{DC} and E_{AC} were calculated for each orbit segment that met the criteria given above. However, there was a problem with the VEFI instrument; the z-axis boom did not unfurl and hence no z-axis data were recorded. This makes it impossible to directly calculate the full values of E_{DC} and E_{AC}. Because the axes refer to the spacecraft orientation it is also not possible to equate the x-axis or y-axis data with specific axes in the Earth-centred

co-ordinate system. Hence in order to progress, a method of approximating the full electric field had to be adopted. The method used is identical to that described in [*Burston et al.*, 2016] and uses

$$E \approx \sqrt{\frac{3}{2}\left(E_x^2 + E_y^2\right)} \qquad [7]$$

where E_x and E_y are the x and y components of the electric field in spacecraft coordinates. The above applies equally to the quasi-D.C. and A.C. data and Eq.[7] was used for both cases. The mean values of E over each orbit segment of interest were calculated for both the quasi-D.C. data and the A.C. data, resulting in a pair of values, $\bar{E}_{DC}$ and $\bar{E}_{AC}$ for each orbit segment. The ratio of each of these pairs of means indicates which process, GDI or KKT, was dominant for each orbit segment.

Results

A total of 1148 DE2 satellite orbit segments met the criteria given in the Method above. They were all recorded during solar maximum conditions using some 550 days of data covering August 1981 to February 1983. There are two sources of error in these measurements. The first is any systematic or random errors associated with the VEFI instrument itself. The second is associated with the technique (Eq.[7]) adopted to estimate the full electric field strength necessitated by the failure of the z-axis component of VEFI. The work of [*Burston et al.* (2016)] estimate that the derived electric field values are generally correct to an order-of-magnitude. Hence, this dominates the intrinsic instrument error, given as 0.1 mVm^{-1}, which can be neglected. A third source of error is also generated by the partial instrument failure: Ideally, the locally horizontal components (in Earth-centred co-ordinates) of both E_{AC} and E_{DC} would be extracted from the data, as only these contribute to driving the GDI and KKT

processes. This is impossible without the z-axis data. The data used here are therefore over-estimates of the actual driving electric fields but probably not to such an extent that the order-of-magnitude estimate is compromised. Comparing the orders of magnitude of the electric field estimates is therefore valid and allows determination of whether $\bar{E}_{DC}$ or $\bar{E}_{AC}$ dominates for each orbit segment examined.

The results show that $\bar{E}_{AC}$ is often similar or larger in magnitude than $\bar{E}_{DC}$, as illustrated in Figure 2. where the mean values of $\bar{E}_{DC}$ and $\bar{E}_{AC}$ for each orbital segment analyzed are plotted against each other as a scatter diagram. Note the difference in scales required for each axis. This is further illustrated in Figure 3., which shows a scatter plot of the ratio of each pair of means, $\bar{E}_{DC} / \bar{E}_{AC}$, for each orbit segment analyzed. In order to clarify how often the GDI is likely to dominate over KKT and vice-versa the ratios were binned by order of magnitude and plotted as a bar chart (Figure 4.). A ratio of order of magnitude < -1 implies $\bar{E}_{AC}$ (KKT) dominance. A ratio of order of magnitude >1 implies $\bar{E}_{DC}$ (GDI) dominance. A ratio of order of magnitude 0 implies that neither dominates the other.

In 34% of orbit segments analyzed show $\bar{E}_{AC}$ and $\bar{E}_{DC}$ to be of the same order of magnitude. Over 60% show clear dominance of $\bar{E}_{AC}$ (KKT). Only 6% show clear dominance of $\bar{E}_{DC}$ (GDI). Hence in 94% (60% + 34%) of cases identified and analyzed by this method, it is likely that if irregularities formed within the patch KKT played a role in their development. Similarly, in 40% (34% + 6%) the DC component may also play such a role.

Conclusions

It is remarkable that the A.C. component of the electric field is comparable to or larger than the quasi-D.C. component in 94% of the orbit segments found that likely traverse large-scale plasma structures in the polar regions. This fact both supports and greatly strengthens the conclusions of [*Burston et al.* (2010)], namely that KKT can be as or more important than the GDI with regard to structuring of patches. The knowledge that KKT can often be as energetic a process as the GDI and can occur anywhere on the patch, rather than in a preferred location (trailing edge) affords a better explanation of the examples observed in [*Kivanc and Heelis* (1997)] of fully structured patches and patches with structure on the leading and trailing edges. In the latter case, there need not have been a complete reversal of the quasi-D.C. component, which seems an unlikely occurrence. Instead, KKT has occurred on the leading edge. In the former case, the KKT allows for an approximate halving of the time it would take to reach complete structuring as irregularities would move in-ward from all directions to the center of the patch, instead of the GDI having to grow across the whole patch diameter.

In order to fully understand irregularity growth in large-scale plasma structures in the polar regions and any associated radio scintillation, it is necessary to go beyond the previously referenced modelling work of [*Gondarenko and Guzdar,* 2006] and include the effects of the A.C. fluctuations in the driving electric field. Addition of the effects of soft particle precipitation in the cusp during patch formation and use of realistic patch geometries derived from radar and Ionospheric Ray Tomography studies would further enhance our understanding.

In addition, detailed knowledge of the power spectra of the electric field values with frequency may determine whether there is a preferential frequency driving the growth of KKT instabilities. In this regard, work by [*Mounir et al.* (1991)], albeit using data from the ARCAD-AUREOL-3 satellite, showed that the power spectrum of the electric field for individual plasma patches followed a power law decay with frequency (with index -1.4 to -1.8). This would indicate, if repeated in general (i.e. the index > -2), that the KKT growth rate may be driven by any A.C. frequency component and there is no preferential frequency range. The A.C. power spectra shown in figure 1. for an example orbit segment tends to back this up. However, the A.C. electric field power spectra averaged over all orbit segments (Figure 5.) shows a steady decrease from 4 Hz to 256 Hz followed by a small increase up to the maximum observed frequency of 1024 Hz, possibly indicating that low and high frequency components are the more important, and that more work is needed.

In addition, in this study we have investigated only KKT and GDI, as these were found to give rise to the greatest growth rates using DE2 data [*Burston* et al. (2016)] and differ only in their response to the quasi-D.C. or A.C. component. However, other instability modes such as CCI could also be present and may need also to be considered.

Acknowledgements

The authors gratefully acknowledge NASA's National Space Science Data Centre (and the Dynamics Explorer scientific team) for the extensive use of DE2 data in this paper. The authors also gratefully acknowledge the support of the Engineering and Physical Sciences Research Council (UK) (Grant EP/H003304/1 "GNSS scintillation: detection, forecasting and mitigation") during preparation of this paper. The data used in this paper comes from the

Dynamics Explorer (DE2) satellite via NASA's National Space Science Data Centre (available at ftp://nssdcftp.gsfc.nasa.gov/spacecraft_data/de/de2/).

References

Basu, S., S. Basu, E. Mackenzie, W. R. Coley, J. R. Sharber, and W. R. Hoegy (1990), Plasma structuring by the gradient drift instability at high-latitudes and comparison with velocity shear driven processes, *Journal of Geophysical Research-Space Physics*, *95*(A6), 7799-+, doi:10.1029/JA095iA06p07799.

Buchau, J., B. W. Reinisch, E. J. Weber, and J. G. Moore (1983), Structure and dynamics of the winter polar capFregion, *Radio science*, *18*(6), 995-1010.

Burston, R., C. Mitchell, and I. Astin (2016), Polar cap plasma patch primary linear instability growth rates compared, *Journal Geophyscal Research-Space Physics*, 121, doi:10.1002/2015JA021895.

Burston, R., I. Astin, C. Mitchell, L. Alfonsi, T. Pedersen, and S. Skone (2009), Correlation between scintillation indices and gradient drift wave amplitudes in the northern polar ionosphere, *Journal of Geophysical Research-Space Physics*, *114*, doi:10.1029/2009ja014151.

Burston, R., I. Astin, C. Mitchell, L. Alfonsi, T. Pedersen, and S. Skone (2010), Turbulent times in the northern polar ionosphere? *Journal of Geophysical Research-Space Physics*, 115, A04310, doi:10.1029/2009JA014813.

Carlson, H. C., T. Pedersen, S. Basu, M. Keskinen, and J. Moen (2007), Case for a new process, not mechanism, for cusp irregularity production, *Journal of Geophysical Research: Space Physics*, *112*(A11), A11304, doi:10.1029/2007JA012384.

Chaturvedi, P. K., M. J. Keskinen, S. L. Ossakow, and J. A. Fedder (1994), Effects of Field Line Mapping on the Gradient-Drift Instability in the Coupled E-Region and F-Region High-Latitude Ionosphere, *Radio Science*, *29*(1), 317-335.

Gondarenko, N. A., and Guzdar (2006), Nonlinear three-dimensional simulations of mesoscale structuring by multiple drives in high-latitude plasma patches, *Journal of Geophysical Research-Space Physics*, *111*(A8).

Gondarenko, N. A., and P. N. Guzdar (2006), Simulations of the scintillation-producing irregularities in high-latitude plasma patches, *Geophysical Research Letters*, *33*(22), doi:10.1029/2006gl028033.

Hargreaves, J. K. (1992), *The Solar-Terrestrial Environment*, Cambridge University Press.

Heppner, J. P., E. A. Bielecki, T. L. Aggson, and N. C. Maynard (1978a), Instrumentation for DC and low-frequency electric-field measurements on ISEE-A, *IEEE Transactions on Geoscience and Remote Sensing*, *16*(3), 253-257, doi:10.1109/tge.1978.294557.

Heppner, J. P., N. C. Maynard, and T. L. Aggson (1978b), Early results from ISEE-1 electric-field measurements, *Space Science Reviews*, *22*(6), 777-789.

Hill, G. E. (1963), Sudden enhancements of f-layer ionization in polar regions, *Journal of the Atmospheric Sciences*, *20*(6), 492-497, doi:10.1175/1520-0469(1963)020

Hunsucker, R., Hargreaves, J.K. (2002), *The High-latitude Ionosphere and its Effects on Radio Propagation*, Cambridge University Press

Jin, Y. Q., J. I. Moen, and W. J. Miloch (2014), GPS scintillation effects associated with polar cap patches and substorm auroral activity: direct comparison, *Journal of Space Weather and Space Climate*, 4, doi:10.1051/swsc/2014019.

Kelley, M. (2009), *The Earth's Ionosphere: Plasma Physics and Electrodynamics*, 2nd ed., 556 pp., Elsevier.

Kelley, M. C., and P. M. Kintner (1978), Evidence for 2-dimensional inertial turbulence in a cosmic-scale low-beta plasma, *Astrophysical Journal*, *220*(1), 339-&, doi:10.1086/155911.

Kintner, P. M., B. M. Ledvina, and E. R. de Paula (2007), GPS and ionospheric scintillations, *Space Weather*, 5, S09003,doi:10.1029/2006SW000260.

Kivanc, O., and R. A. Heelis (1997), Structures in ionospheric number density and velocity associated with polar cap ionization patches, *Journal of Geophysical Research-Space Physics*, *102*(A1), 307-318.

Linson, L. M., and J. B. Workman (1970), Formation of striations in ionospheric plasma clouds, *Journal of Geophysical Research*, 75(16), 3211–3219, doi:10.1029/JA075i016p03211.

Mounir, H., C. J. Cerisier, A. Berthelier, D. Lagoutte, and C. Beghin (1991), The small-scale turbulent structure of the high latitude ionosphere: ARCAD-AUREOL-3 observations, *Ann. Geophys.*, 9, 725–737.

Oksavik, K., J. Moen, M. Lester, T. A. Bekkeng, and J. K. Bekkeng (2012), In situ measurements of plasma irregularity growth in the cusp ionosphere, *Journal of Geophysical Research-Space Physics*, *117*, doi:10.1029/2012ja017835.

Ossakow, S. L. and P. K. Chaturvedi (1979), Current convective instability in the diffuse aurora. *Geophys. Res. Lett.*, 6: 332-334. doi:10.1029/GL006i004p00332.

Sojka, J. J., M. V. Subramanium, L. Zhu, and R. W. Schunk (1998), Gradient drift instability growth rates from global-scale modeling of the polar ionosphere, *Radio Science*, *33*(6), 1915-1928.

Weber, E. J., J. Buchau, J. G. Moore, J. R. Sharber, R. C. Livingston, J. D. Winningham, and B. W. Reinisch (1984), F-layer ionization patches in the polar-cap, *Journal of Geophysical Research-Space Physics*, *89*(NA3), 1683-&, doi:10.1029/JA089iA03p01683.

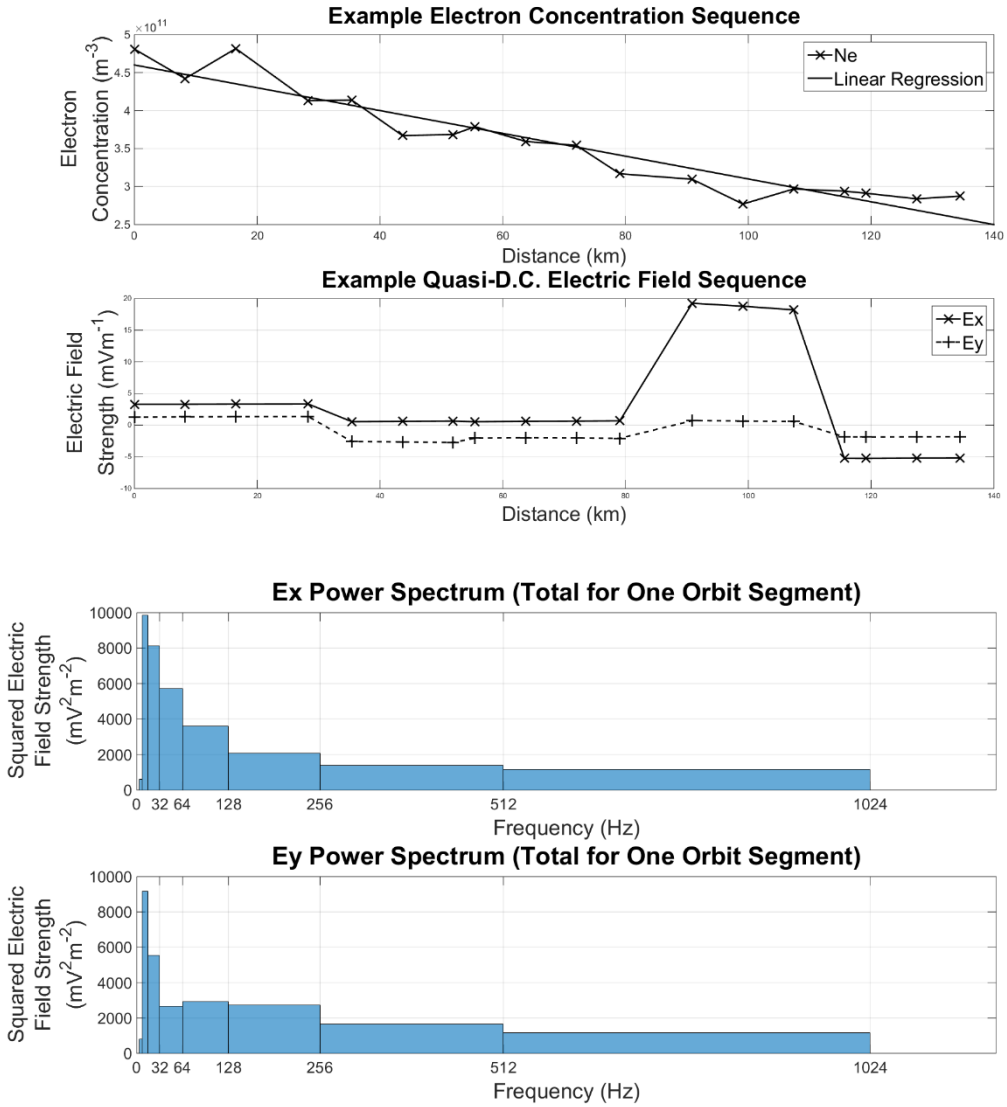

Figure 1. The electron density, D.C. electric field (x and y) components and the power spectra of the (x and y) components of the A.C. electric field for an example orbit segment that satisfies the three required criteria (magnetic latitude, height and gradient).

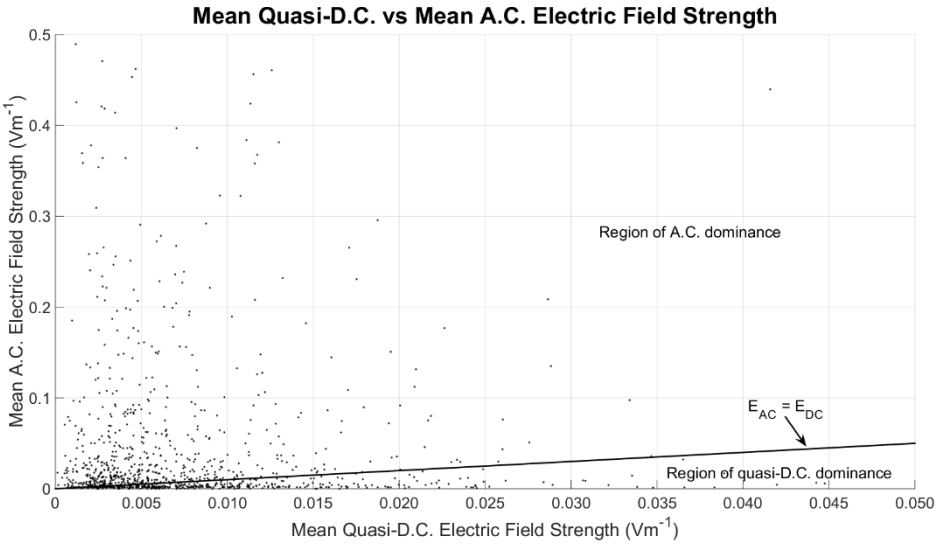

Figure 2: The mean quasi-D.C. electric field strength plotted against the mean A.C. field strength for each orbit segment. Note the difference in scales on each axis.

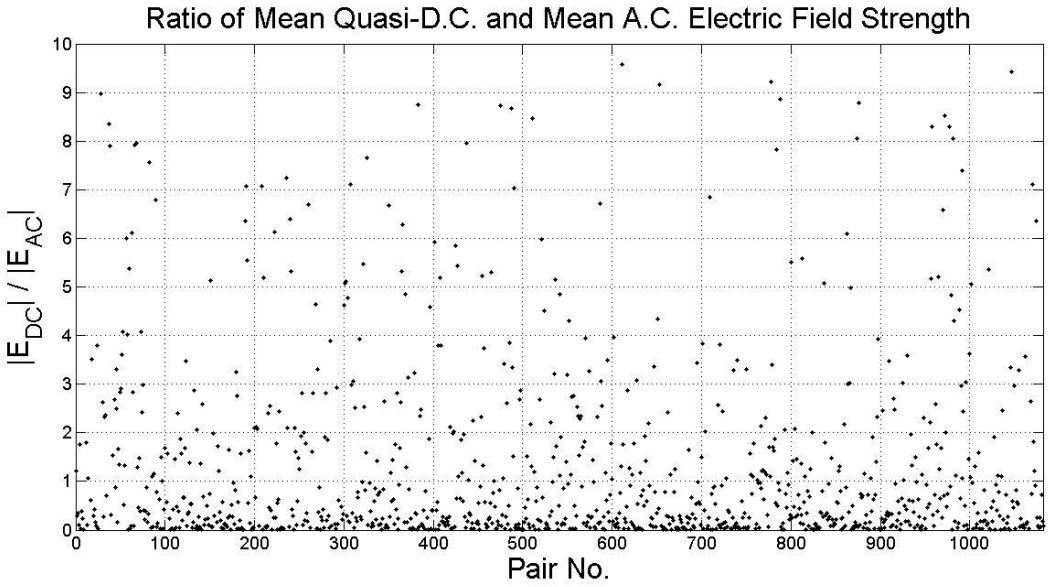

Figure 3: Scatter plot of the ratio of each pair of means, E_{DC}/E_{AC}, for each orbit segment analyzed.

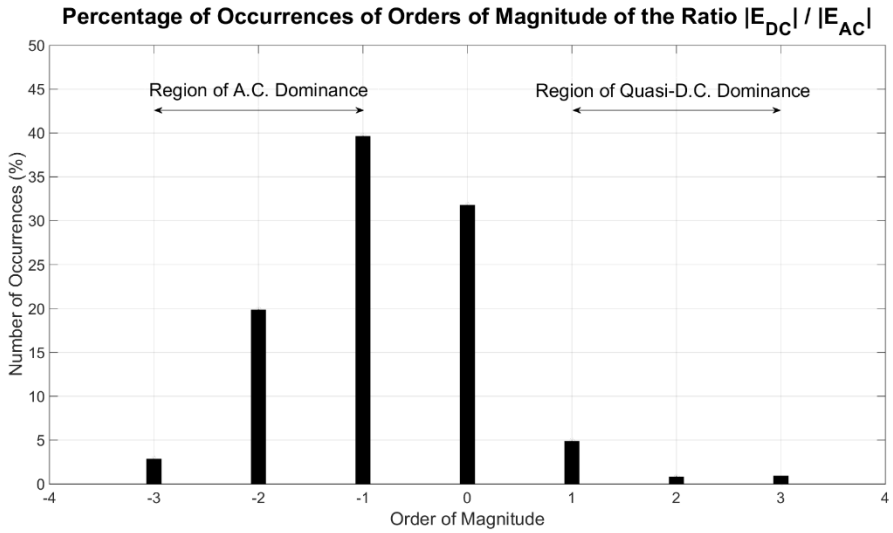

Figure 4: The occurrence of orders of magnitude of the ratio, E_{DC}/E_{AC}, expressed as a percentage of the total number of orbit segments analyzed. A ratio of order of magnitude $\leq$-1 implies E_{AC} dominance. A ratio of order of magnitude $\geq$1 implies E_{DC} dominance. A ratio of order of magnitude 0 implies that neither dominates the other.

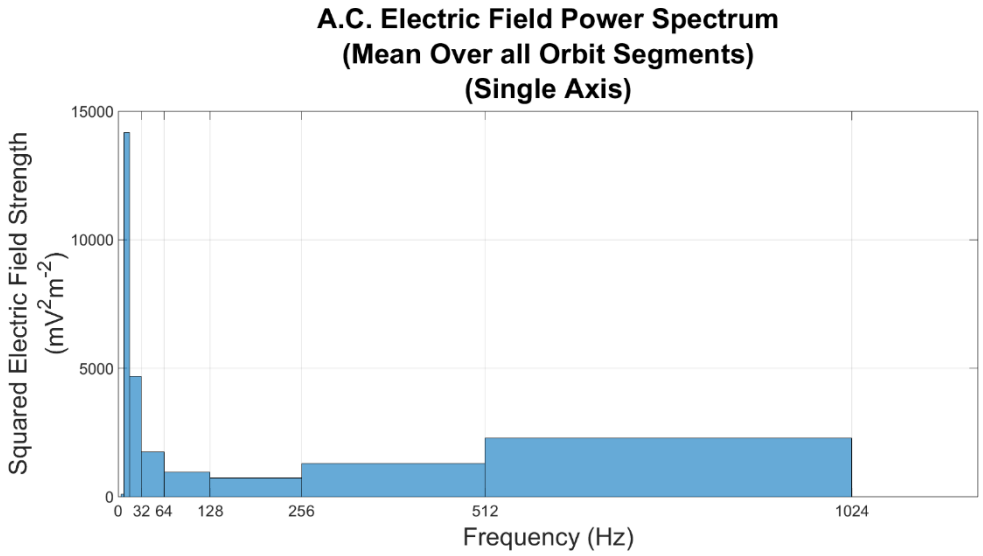

Figure 5. The average power spectrum for all orbit segments used in this study, that meet the required magnetic latitude, height and density gradient.